

# Design, construction and utilization of a university plasma laboratory

W. Gekelman<sup>1</sup>✉, P. Pribyl<sup>1</sup>, Z. Lucky<sup>1</sup>, S. W. Tang<sup>1</sup>, J. Han<sup>1</sup>  
and Y. Qian<sup>1</sup>

<sup>1</sup>Department of Physics and Astronomy, University of California at Los Angeles, 90095, USA

(Received 10 March 2020; revised 27 May 2020; accepted 29 May 2020)

We present the elements required to construct two devices used in an undergraduate plasma physics laboratory. The materials and construction costs of the sources, the vacuum systems and probe drives and electrical circuits are presented in detail in the text and the first appendix. We also provide the software for probe motion and data acquisition as well as the electrical schematics for key components. Experiments which have been performed are listed and two (resonance cones and whistler waves) are described in greater detail. The machines are flexible and original research is possible.

**Key words:** plasma devices, plasma diagnostics, plasma properties

---

## 1. Introduction

Plasma physics is an area that encompasses many-body nonlinear systems. It is interesting from a basic physics standpoint as it involves interacting waves found nowhere else, turbulence, transport and transition to chaos among many other things. It is a field with many applications, such as harnessing thermonuclear fusion as an energy source but there are many more applications. Low temperature industrial plasmas are used to manufacture most semiconductor based circuits such as CPUs, digital memory devices and a wealth of other devices. Without it there would be no cell phones, powerful laptops and the hundreds of sensors and chips built into modern cars, jets and cameras within them. Plasmas are also used in medicine, agriculture, cutting and hardening metal, sterilization, etc. and the list is enormous. A first rate laboratory course for college juniors and seniors is an essential part of a curriculum in a university with a program in this area.

Laboratory experience is very important for a student who is interested in going into the field of plasma physics or an associate engineering area in the future. While undergraduates are usually encouraged to find and work for a research group, it is always hard as the number of available spots, and the amount of time spent by researchers in training them, is limited. University laboratory courses on the other hand, provide opportunities for a larger number of students to be involved in experimental research. With such motivation, laboratory courses offering students fundamental knowledge of plasmas have been offered among institutions since the last century. A course consisting of DC/RF (direct current and radio frequency) breakdown,

✉ Email address for correspondence: [gekelman@physics.ucla.edu](mailto:gekelman@physics.ucla.edu)

shockwave and various other experiments has been offered in Stanford University since 1966 (Crawford & Ilic 1976). At Acadia University, Maclatchy described a low-cost laboratory experiment using a propane burner (Maclatchy 1977). An elementary plasma experiment using commercially available gas tubes was designed by Alexeff *et al.* to serve for lower division undergraduate laboratory courses (Alexeff, Pytlinski & Oleson 1977). Other universities have also offered laboratory courses featuring plasma etching with microelectronics (Fleddermann 1997), a DC glow discharge (Wissel *et al.* 2013) and plasma surface interactions (Kabot *et al.* 2016).

While the above courses provide students with an introductory knowledge about plasma, most of the devices offered for undergraduate level are simplified for educational purposes. Yet, undergraduates, especially junior and senior students, have the ability and potential to handle courses that are much more complicated. Students, especially physics majors, need knowledge in designing the experiment, understanding the diagnostics, comprehending the data and writing up the results in a research paper. This is hard to accomplish if courses are made easier and easier in the undergraduate curriculum. Here we offer one example; the design and construction of an undergraduate plasma physics laboratory at the University of California, Los Angeles, where the course (Physics 180E plasma lab) targets junior and senior undergraduate students.

The plasma laboratory currently has two devices designed to host complementary experiments. These devices are capable of replicating classical plasma physics experiments such as whistler wave generation, or even serve real research purposes. However, any laboratory requires a capital investment, and at a minimum the machines must be constructed or purchased. The machines described here require vacuum systems, turbomolecular pumps and mechanical pumps, vacuum gauges to measure the chamber pressure, gas feeding systems, plasma sources as well as diagnostics. Data acquisition is performed utilizing a computer programmed automated system written in Python (see appendix 2, see supplementary movie <https://doi.org/10.1017/S002237782000063X>). The Python code controls stepping motors for probe motion, collects data from the oscilloscope and archives them to disk. Once the data are stored on the auxiliary computers, generally inexpensive computers such as laptops are needed to process it and create graphics and movies.

During the course, students have full control over various experimental set-ups. They apply the knowledge acquired from theory classes to experiment scenarios, learn about data presentation in multi-dimensions and write laboratory reports that resemble short publications in refereed journals. Students collaborate in a research setting by working in groups of 2 or 3. At the end of the course, each group presents their result to an audience, simulating a conference or workshop environment. Such a laboratory course not only bequeaths the students with the appropriate experimental training, but also allows them to find out if hands on, team-based work, giving presentations and especially scientific research is a suitable career path for them.

The manuscript is organized as follows: § 2 describes two types of machine set-ups and construction – inductively coupled plasma (ICP) and the twin cathode device. Section 3 illustrates the probe drives and diagnostics. We discuss their design and cost of fabrication. Section 4 provides the course organization and experiments based on a 10 week quarter system. Section 5 discusses laboratory safety. A summary is provided in § 6. Construction of a laboratory involves costs, and these are outlined in appendix 1 using U.S. dollars in 2020. The funds for setting up a state of the art undergraduate laboratory are considerable and physics departments must look at them as the cost of hosting an outstanding undergraduate program.

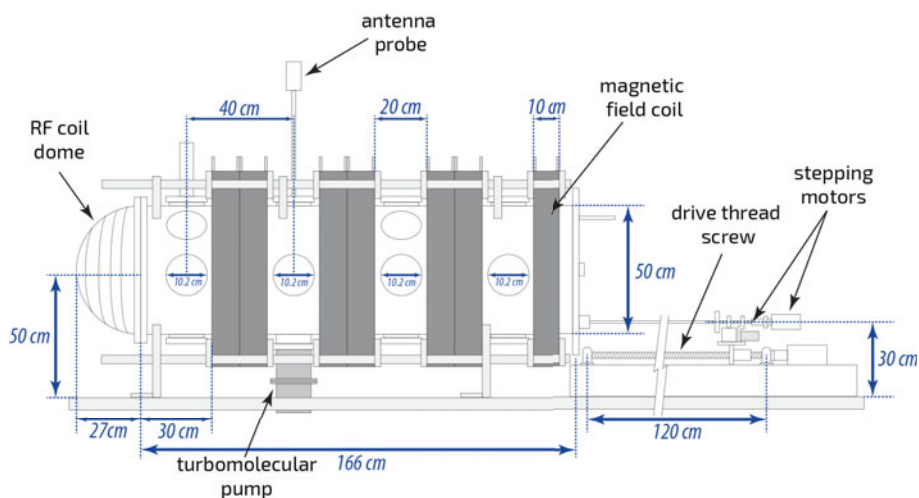


FIGURE 1. Schematic diagram of the ICP plasma source showing several key components.

## 2. Machine design and construction

### 2.1. ICP Device

The first device is powered by a pulsed inductively coupled plasma source, which is shown in figure 1. It is approximately two metres in length with a ceramic dome antenna on one end. The dome (shown on the left of figure 1) contains a 32-turn water-cooled copper coil. The plasma leaves the source and flows into the chamber surrounded by magnetic field coils. The dome used was a ‘Novellus Speed Dome’. They are no longer manufactured but used versions can be purchased on the surplus market. Instead of a dome, a differently shaped glass or ceramic chamber with a coil wound on the outside can be used. In one iteration, a thick-walled glass cylinder approximately 8 inches long<sup>1</sup> and 6 inches in diameter had 5 copper turns wrapped around it as the antenna, and made a very intense plasma with a few kilowatts of RF.

The ICP uses a dome-shaped antenna shown on the left. The plasma leaves the source and flows into a single chamber surrounded by magnetic field coils. The end flange opposite the dome is an aluminium disk with a 6 inch viewport and a small port on the bottom to allow the probe to access the chamber. There are three additional 2 inch ports on the end flange which can also be used as viewports and for probe access. The flanges have a bolt circle and O-ring grooves to provide interchangeability of components such as allowing windows to be placed on them. A photograph of the device is shown in figure 2. The breakout of costs of constructing the chamber, flanges and frame are in appendix I. The construction based on reasonable estimates of materials and labour is approximately \$13 000.

The chamber was made from a 3/16 inch thick 304 stainless steel sheet. The purchased sheet was 6 feet long and 75.4 inches wide. The sheet was rolled and welded to form a tube. One could buy a ready-made tube but it is far more expensive. The cylinder was placed on a horizontal mill and 16 holes for the ports 4.25 inch in diameter were cut into it. For the port extensions, standard thick-wall stainless tubing with a 4 inch inner diameter was sliced into 2 inch long sections. The tubes were

<sup>1</sup>Dimensions of raw materials purchased are called out in inches as this is how they are ordered. The experimental parameters are given in metric units.

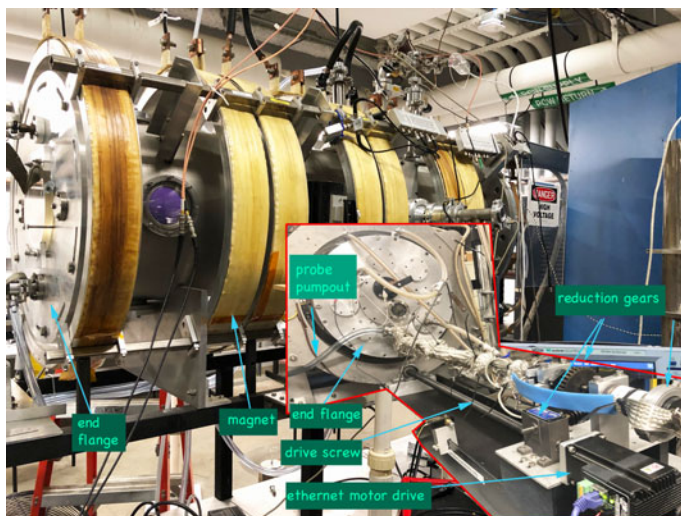


FIGURE 2. Photographs of the ICP plasma device and outlined in red the probe drive at the rear end of the device. The probe travels in/out of the device through a double ‘O-ring’ seal. A probe pumpout line driven by a mechanical pump removes any air that makes it past the first O-ring. An ethernet motor drive/controller rotates the screw drive. A second motor drive (not visible) rotates the probe enabling data acquisition on two-dimensional planes. The inset in red shows a nearly identical probe drive on the dual cathode device.

then vacuum welded to the chamber (figure 2) followed by flanges welded to the tubes (also shown in figure 2). The flanges have a bolt circle and O-ring grooves to provide interchangeability of components such as allowing windows to be placed on them. One specialized port has an extension tube for clearance past the magnets to allow the attachment of a turbomolecular pump.

The plasma device includes seven magnet coils wound from  $1/4 \times 3/4$  inch formvar insulated rectangular copper bars which have transformer paper insulation interleaved between the layers of turns. These were wound on rolled aluminium  $4 \times 1.5$  inch U-channel. Each coil formed a ring that would fit over the chamber and flanges with the ends welded for rigidity. The uncooled magnets produced an axial magnetic field that may be varied up to 150 Gauss.

The operating frequency of the ICP source is 600 kHz with up to 5 kW available power. At full power there is 4 kV across the 32-turn coil, but only 10 turns of the largest diameter are powered between the open end of the dome and a grounded tap. It is key that the ground potential is not at the end of the coil. The remaining turns are inductively coupled to the driven set and have an induced RF voltage. Operation in this pseudo-balanced configuration was important to avoid accelerating plasma down the chamber; an early test with the end of the coil grounded heated the glass window at the opposite end of the machine to  $60^\circ\text{C}$ . The source has run daily for over seven years without failure. It may run continuously, but is typically pulsed at 10 Hz with an ‘on’ time of 10 ms. The rapidly time varying magnetic field in the external coils produces an azimuthal electric field in the dome which accelerates electrons and partially ionizes the gas. The source operates best in a magnetic field free region, therefore the first magnet is 30 cm away from the coils. In typical repetition rates and duty cycles (e.g. 10 Hz, 10%), there is residual plasma from the previous pulse

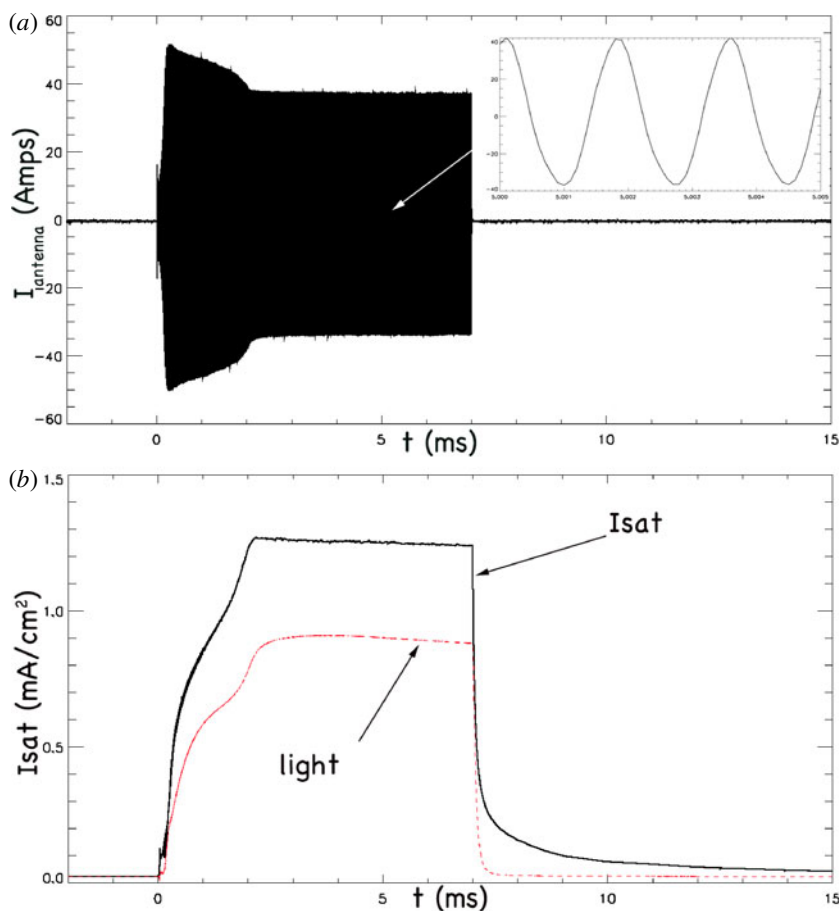


FIGURE 3. (a) The current (in Amperes) in the ICP antenna during one pulse of the ICP device. The inset shows approximately 2.5 cycles of the 600 kHz current. The peak-to-peak RF voltage on the antenna is of order 300 V. (b) The black curve is the ion saturation current measured by a small disk probe at the centre of the plasma column. The red curve is light recorded by a photodiode (arb units).

in the chamber and the ionization of neutrals occurs rapidly. The plasma streams out of the source region and fills the chamber within 2 ms after switching on. The ICP operates best in the pressure regime 0.3–10 mTorr in argon and, and 3–20 mTorr in helium. Gas is fed using a 100 sccm (standard cubic centimetres per second) mass flow controller. At 0.5 mTorr, the plasma is weakly ionized (of order 1%). Pulsed RF power supplies to drive the coil are commercially available (see appendix 1).

Figure 3 shows the RF current for one pulse of the ICP source as well as the light recorded by a photodiode positioned at one of the windows. The light vanishes in tens of microseconds after the RF is terminated because the primary electrons vanish, however, the density decays much more slowly, in tens of milliseconds.

While the source is energized, many diagnostics are contaminated by the RF noise and thus experiments are typically performed in the quiescent afterglow. During this time density fluctuations are low, with  $\delta n/n < 1\%$ . After the driven phase of the plasma is terminated the plasma decays from  $n \simeq 2 \times 10^{11} \text{ cm}^{-3}$  to  $10^9 \text{ cm}^{-3}$

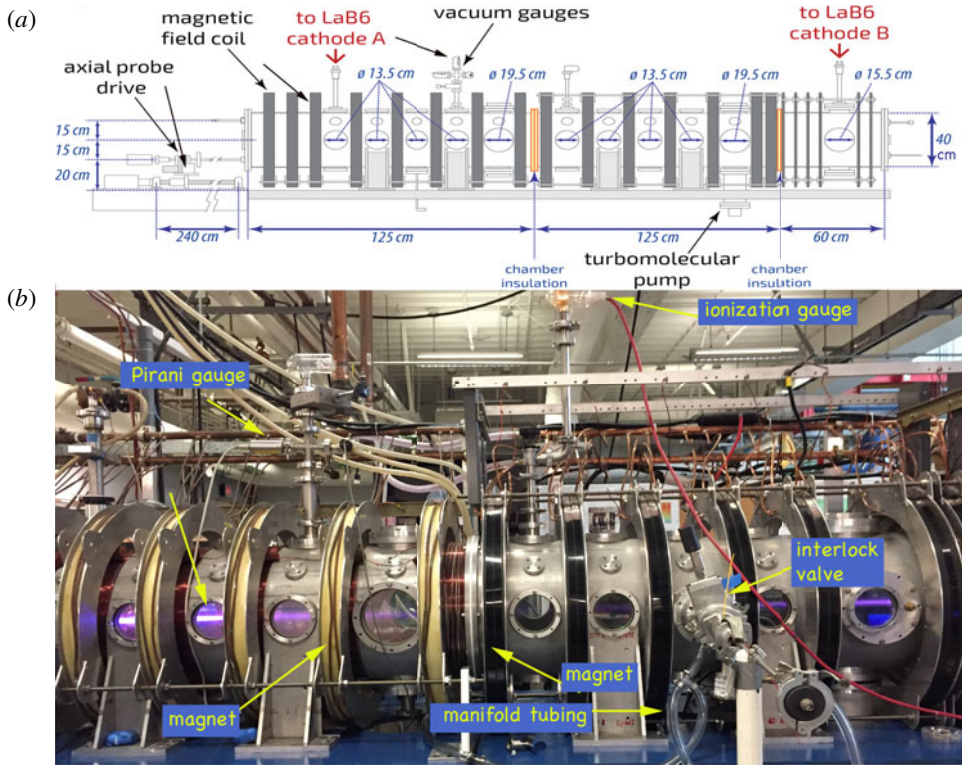


FIGURE 4. Twin cathode device which produces plasma with a DC discharge. (a) Schematic view of vacuum system illustrating an axial/radial probe drive on the left, the magnets and ports. (b) Photograph of the machine with several elements highlighted. There are cathode plasma sources at both ends and a plasma column is visible.

in 30 ms. This is seen in the ion saturation current curve in figure 3(b). The ion saturation current,  $I_{\text{isat}}$ , is proportional to  $n\sqrt{T_e}$ . The electron temperature is 3 eV during the discharge and decays to 0.5 eV in 200  $\mu\text{s}$ , after which it continues to decay slowly. The rapid initial decay of  $I_{\text{isat}}$  is due to the fast drop in  $T_e$ . The subsequent decay follows that of the density. The electron temperature was determined from the characteristic  $I-V$  curves obtained during a voltage sweep of the Langmuir probe during the discharge and at several times in the decay. The density was determined by calibrating the Langmuir probe results with a microwave interferometer. Experiments such as whistler wave studies are performed on a time scale of tens of nanoseconds at varying delay times in the afterglow. At any one delay time the density and temperature are essentially constant.

## 2.2. Twin cathode device

The second plasma machine in the laboratory is complementary to the first. It uses two hot Lanthanum Hexaboride ( $\text{LaB}_6$ ) cathodes as sources of electrons for two independent DC discharges. A schematic and photograph of the device is shown in figure 4.

The DC discharge utilized three chambers which are shown in figure 4(a). There are two half-chambers connected with an insulating gap that were acquired from a

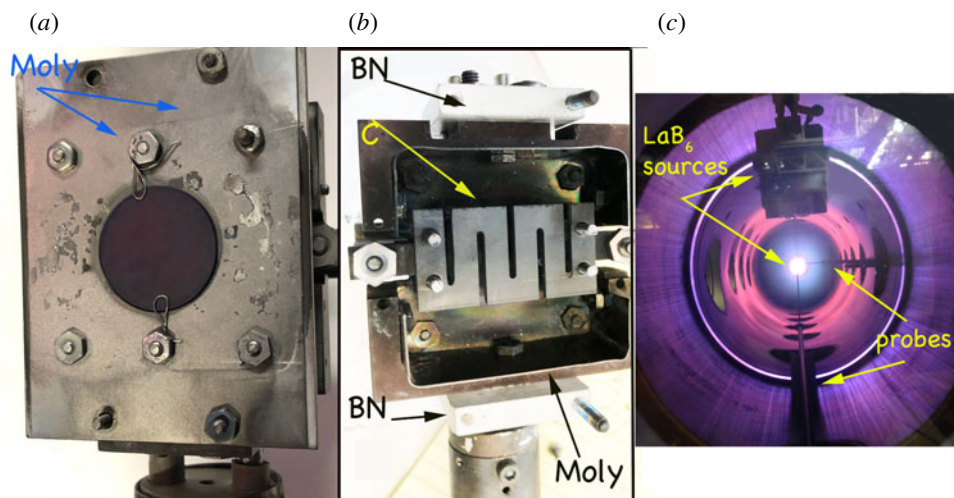


FIGURE 5. Photographs of the small  $\text{LaB}_6$  source used in the twin cathode DC discharge device. (a) Front view showing  $\text{LaB}_6$  cathode in the centre with a molybdenum in the centre with a molybdenum heat shield in front of it. All the screws and nuts are made of molybdenum. Stainless steel will melt at the  $\text{LaB}_6$  operating temperature. (b) A carbon heater which is placed directly in back of the cathode. The cathode is placed in a Moly box. All insulators are made of boron nitride (BN). (c) A view from end of chamber showing the placement of the two cathodes and two probes. The axial and transverse probes are on computer motion-controlled stages. The cost of constructing the carbon-moly oven for the  $\text{LaB}_6$  is approximately \$750. Details are in appendix 1.

previous laboratory device. Each aluminium (6061-T6, vacuum weldable) half-chamber is 48 inches long and has a 0.2 inch wall and an inner diameter of 16 inches. A third chamber similar to the two half-chambers but 24 inches long is attached to the right end of the device. The chambers are ‘floated’ electrically from one another using Teflon ring separators between them. This enables operation as a magnetized double plasma device. The turbo pump is also electrically isolated from the chamber with a Delrin spacer. This is necessary if we need to bias the chamber, as the body of the turbo pump is at ground potential. The chamber flanges have O-ring grooves and the Teflon insulators are flat. The magnets were wound on a simple welded Aluminium mandrill from number 10 magnet wire (good to 35 Amperes). Since the chambers were fabricated at different times the ports are not all identical.

The plasma sources for the DC discharge are based on  $\text{LaB}_6$  which has a high electron emissivity at 1600–1700°C and can produce plasmas of density up to  $10^{12} \text{ cm}^{-3}$  in this device. The sources are small and the resulting plasma column is about 3 cm in diameter. Larger sources can be used, but the heat load would require cooling shrouds inside the chamber to prevent the chamber walls from becoming too hot to touch. Figure 5 has photographs of the cathode assembly. A computer aided design (CAD) drawing and temperature profiles of the various elements from a COMSOL™ simulation are shown in figure 6.

### 2.3. Vacuum systems

The vacuum systems of both devices consist of small (Osaka Vacuum Systems, TG1300MBWB, 1300 liters/sec, mag-lev) turbomolecular pumps backed by 16 CFM

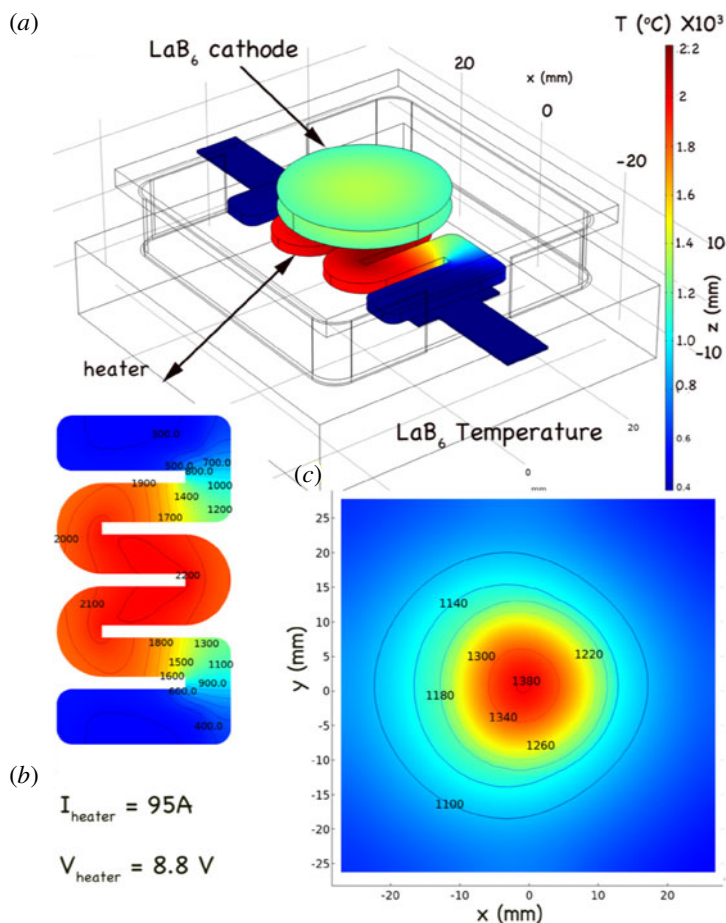


FIGURE 6. A drawing of the cathode (a) with contour plots predicting the temperature of the heater and cathode (b,c) and calculated using COMSOL™. The heater and cathode are mounted in a carbon box with a 1 mm thin layer of molybdenum. The reflection coefficient of molybdenum for photons in the infrared was estimated as 0.2. The carbon heater is machined on a CNC mill. The centre of the cathode is at 1380°K. For cathode operation at 1700°K, the current required is  $I_{\text{heater}} = 120\text{ A}$ ,  $V_{\text{heater}} = 12\text{ V}$ .

(cubic feet per minute) mechanical pumps. Both systems can reach a base pressure of  $1 \times 10^{-6}$  Torr several hours after being open to air. The combination of the pumps costs approximately \$23 K. A spreadsheet with approximate cost (in 2020 dollars) of all components is in appendix I. Each system has a second mechanical pump attached to a manifold with 6–8 valves. These pump-out systems operate at pressures of about 20 mTorr. Flexible vacuum tubing from the manifold is used to continuously pump the double central plenum of the sliding seals as probes are moved. This roughing system is also used to pump down interlock chambers ('air locks') which are used to remove probes or introduce them to the systems without letting them up to atmosphere. The ICP source is tolerant to bursts of pressure and can operate in oxygen. The cathode sources can stand the brief pressure bursts which occur when the interlocks (at <50 mTorr) are opened to the machine. The chamber pressures are

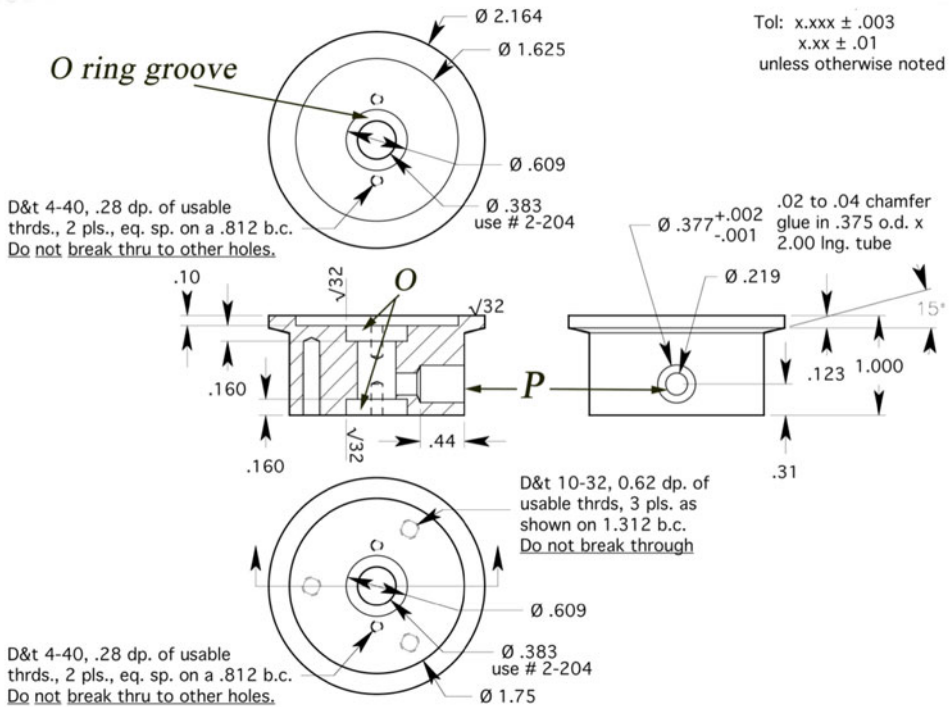


FIGURE 7. A technical drawing for a feedthrough for a 3/8 inch probe shaft. The components labelled 'O' are grooves for Viton™ O-rings. When the probe is moved, any air that gets by the first O-ring is pumped out of the receptacle marked P. A 2 inch tube is glued into 'P' and is maintained under vacuum by a mechanical pump with a base pressure of about 20 mT. A 6 cubic feet per minute (CFM) pump is attached to a manifold which can service all of the feedthroughs on each device. Each line on the manifold has an inexpensive shutoff valve to allow probes to be interchanged.

monitored with ionization gauges and a Pirani gauge, while the foreline and manifold pressures are monitored with convectron gauges.

### 3. Diagnostics capabilities

We illustrate some of the diagnostics employed as well as device features which allow for smooth machine operation.

#### 3.1. Sliding seals

A double sliding seal allows probes and antennae to be moved in/out of the device without introducing bursts of air. Drawings of the sliding seal components are shown in figure 7.

#### 3.2. Probe drives

Both devices are equipped with axial probe drives capable of motion along the magnetic field ( $z$  direction) and rotation on an arc through the centre of the device. The  $z$ - $\theta$  axial probe drive is shown in figure 8(a). It has a right-angle bend and is capable of moving the probe along the magnetic field ( $z$ -direction) and rotating

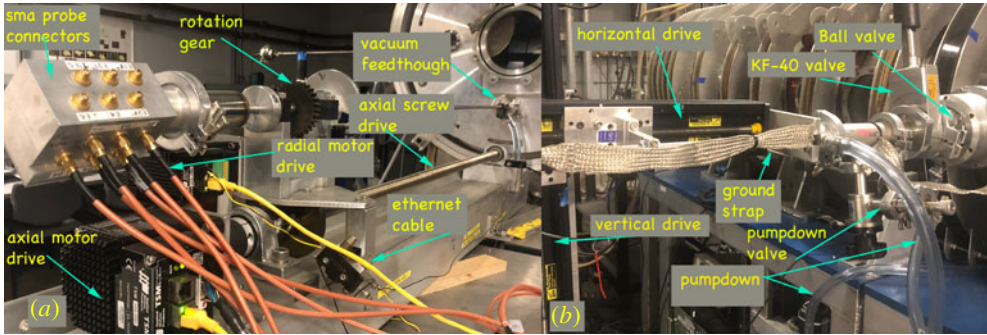


FIGURE 8. (a) Axial probe drive on ICP device. The 2 Ethernet controlled motors are shown. The connector box at the upper left has 12 SMA connectors. Six are for differentially wound pickup loops for the B-dot probe (two connectors for each axis) and six more for the six arms of a three axis electric dipole probe. There is a differentially pumped vacuum feedthrough. A drive screw is for axial (in/out) motion and a set of gears attached to a second stepping motor controls rotation. (b) The transverse probe drive on the dual cathode device. Two sets of motors control the up-down and in/out motion. A ball valve is attached to a KF-40 valve on the right.

the tip of the probe through an arc that passes through the centre of the device ( $\theta$ -direction) as diagrammed in figure 9. This probe is capable of rotating until it touches the walls of the chamber, but the typical operating maximum rotation angle is  $\theta_m = \pm 30^\circ$ . It maps out an arced surface which is projected onto an  $x$ - $z$  plane (the  $z$ -axis is parallel to the background magnetic field), with the centre of the arc typically  $\sim 2.5$  cm higher than that at the ends.

The original data acquisition system was based on LabVIEW™ software, had compatibility issues with certain devices which made it unnecessarily complicated for students in a teaching laboratory to learn and operate, as well as instability issues. That package used National Instruments stepping motors, motor controllers and computer interfaces, all of which were very expensive (cost per drive axis  $\sim \$7000$ ). We chose to switch to Python (which is free and open source), and bought commercial stepping motors that have onboard controllers with Ethernet communication and can be run off inexpensive power supplies (Applied Motion Products: TSM34Q-1DG for axial drive and STM 23S-3EE for rotation). The present system costs about \$250/channel (primarily determined by the price of the motor).

Probe drives capable of vertical ( $x$ - $y$ ) motion were also implemented to move probes on planes transverse to  $B_z$ . Vacuum compatible ball valves designed in house (Leneman & Gekelman 2001) were implemented to allow the probes to track the motor motion without the use of bellows type vacuum connections. There are two sets of drives that are used on each device: a  $z$ - $\theta$  axial probe drive and a  $x$ - $y$  transverse probe drive. These are pictured in figure 8(b).

A number of probes are typically inserted in the transverse plane ( $x$ - $y$ ) access port, such as B-dot or Langmuir type diagnostics. The transverse probe is changed by (a) dismantling the old probe from the drive, (b) closing the KF-40 valve and letting the air-lock volume up to air (c) inserting a new probe and pumping it down to 100 mTorr with a mechanical pump via the pump-down valve and (d) opening the KF-40 valve and reattaching the probe to the drive. This is done with the ICP source or DC discharge switched off. The LaB<sub>6</sub> cathode is insensitive to small amounts of

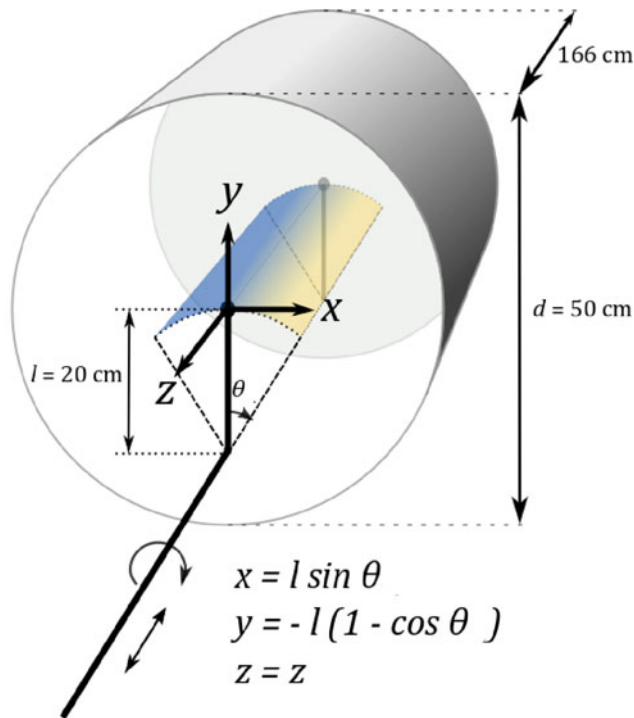


FIGURE 9. Schematic of the probe motion attached to the axial probe drive, applicable to both machines. The probe enters the chamber through an opening a distance  $L$  below the centre of the machine such that the probe tip is at the machine centre when vertical.  $L = 20$  cm for ICP,  $L = 15$  cm for twin cathode device. The probe has two degrees of freedom: it can move in and out of the chamber (along  $z$ ) or rotate about its offset axis. The probe tip sweeps an area on a curved surface of a cylinder as indicated by the graduated colour surface. The general coordinate transform from probe coordinates ( $L, \theta, z$ ) to machine coordinates ( $x, y, z$ ) defined from the centre of the machine is shown.

air and will recover its emission in a few minutes. In contrast, the axial probes with a right-angle bend require the machine to be let up to air to replace them.

The data acquisition (DAQ) computer running the software moves the probes independently, displays their current position (and previous positions in a data run) and controls the oscilloscope used to acquire data. At each probe position data are averaged and recorded using an oscilloscope as a digitizer. The software then reads the temporal data from the scope and writes those and the probe position to a file in the PC. The data are written in hdf5 format. Both Python and IDL programs are provided to the students to be able read the files once the data run is complete.

### 3.3. Probes

Measurement of the plasma density is required for all experiments. Langmuir probes (Chen, Etievant & Mosher 1968; Hershkowitz 1989) have long been the staple of experimental plasma physics (Mott Smith & Langmuir 1926) and although they are not terribly accurate, they are easy to build and use. One can purchase Langmuir probes and probe sweepers from several vendors but they can be quite expensive.

Instead, we build our own probes and use a relatively inexpensive probe sweep circuit shown in appendix 3. An arbitrary waveform generator (e.g. Agilent 33220A, 20 MHz) drives a homemade amplifier which can sweep over 100 Volts and deliver a current of 3 A. This powers the probe which is usually a 2 mm diameter disk of tantalum. We do not use a cylindrical probe for the teaching portion of this laboratory because the ‘knee’ in the  $I$ - $V$  curve is better defined for a planar probe (Hershkowitz 1989), and we are not investigating electron energy distribution functions in detail but only the electron temperature and ion saturation current. A typical  $I$ - $V$  curve is shown in figure 10(a) and the plasma density on a plane transverse to the axial magnetic field (100G) is shown in figure 10(b). The electron temperature profile during the DC discharge in the twin cathode, LaB<sub>6</sub> machine ( $V_D = 120$  V,  $I_D = 20$  A) is shown in figure 11. In this case, the probe was moved to 1334 positions in the  $x$ - $z$  plane ( $z$  is along the magnetic field direction and points at the source) and at each position, 25 current and voltage waveforms are acquired and averaged. As Langmuir probes are not accurate for density measurements, we used a 60 GHz microwave interferometer based on a Gunn diode and horn to calibrate the probes. Details of the interferometer developed by Gilmore may be found in Gilmore *et al.* (2002).

The plasma potential can be calculated using the  $I$ - $V$  characteristic of the Langmuir probe, but in a second experiment an emissive probe (Sheehan *et al.* 2011) was used to measure it directly. The electric field was determined by  $\mathbf{E} = -\nabla V_p$ . When the electric field is known the plasma  $\mathbf{E} \times \mathbf{B}$  drift can be computed. These are shown in figure 12 for the twin cathode device.

The whistler wave experiment records the wave magnetic field with loop probes sensitive to  $\partial \mathbf{B} / \partial t$ . Magnetic loop probes have been utilized for decades (Gekelman *et al.* 2011). Their construction and calibration procedures have become sophisticated over the years, but the basic principle of operation is Faraday’s law. Electric dipole probes are used to measure the resonance cones (which are electrostatic) and are described in figure 14.

Another experiment utilized a Mach probe (Hutchinson 2002) which consisted of two small back-to  $\mathbf{E} \times \mathbf{B}$ -back planar probes separated by an insulator. Ion saturation current was collected from each face. The probes were oriented transverse to the main field, i.e. perpendicular to the background magnetic field,  $\mathbf{B} = B_o \hat{z}$ . At 85 Gauss the ion gyroradius is 4.5 cm, which is much larger than the size of the collector ( $A = 2$  mm<sup>2</sup>) and the ions are essentially unmagnetized on the scale of the probe. Consider a small, single-sided disk probe (probe 1) collecting ion saturation current when ions are drifting towards the probe with velocity  $V_D$ . The current to the probe is  $I = neA(c_s + V_D)$ . Here,  $c_s$  is the sound speed,  $n$  is the density and  $A$  is the probe area. A second single sided probe with the same area faces in the opposite direction. Under these conditions the ratio  $(I_1 - I_2)/(I_1 + I_2) = (ne[(c_s + V_D) - (c_s - V_D)]/ne[(c_s + V_D) + (c_s - V_D)]) \simeq (v_D/c_s) = M$  is approximately the Mach number. The analytic expression given by Hutchinson (Hutchinson 2002) is  $I_1/I_2 = e^{KM}$ . The value of  $K$  has been debated (Kuehl 1962) but is of order 1.3. For Mach numbers smaller than 1 both expressions give similar results. The Mach probe was set up to measure flow along  $z$  and  $y$  so that a direct comparison to figure 12(a,b) cannot be made. However, the vertical component of the Mach number is in agreement with the magnitude of the flow velocity. Figure 12(c) illustrates the vertical Mach number on the transverse plane.

#### 4. Course organization and experiments

The UCLA course hosts up to 15 students for each 10-week quarter that it is taught. There is a weekly two-hour lecture on the following week’s experiment.

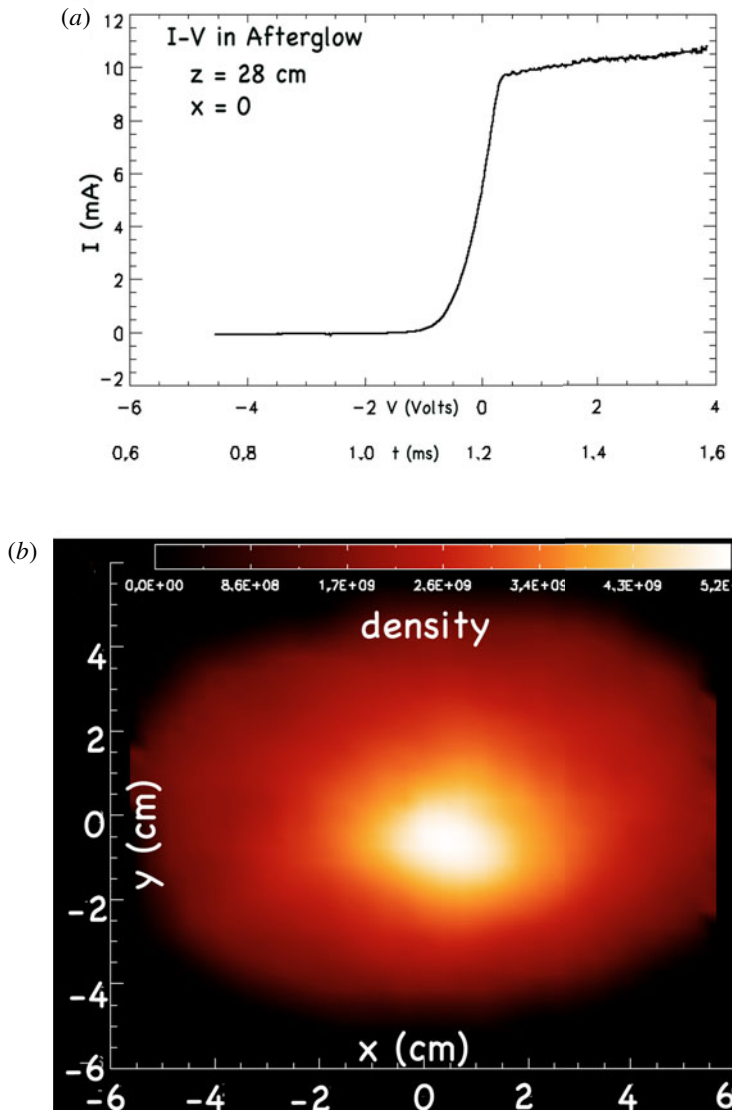


FIGURE 10. (a) Sample Langmuir characteristic  $I$ - $V$  curve acquired in the afterglow of the twin cathode DC discharge plasma. The transition of the curve was swept in  $100\ \mu\text{s}$  and the knee is clearly visible. The probe was a 3 mm diameter disk and the resistor used was  $100\ \Omega$ . Time  $t = 0$  is the start of the afterglow.  $B = 100\ \text{G}$ ,  $P = 0.7\ \text{mT}$  in argon. The density is  $4 \times 10^{11}\ \text{cm}^{-3}$ . The density in the afterglow of (b) can be made arbitrarily small by triggering the diagnostics at the appropriate time. (b) Plasma density in a plane in the afterglow plasma. Data were acquired at 961 spatial positions. The  $I$ - $V$  curve was swept and ten sweeps were averaged at each location.

When the lecture is over, the students go to the laboratory for a demonstration of the equipment to be used, to observe the working experiment and to get a sense of the data by watching waveforms on oscilloscopes. The experiment is then disassembled. Each group of two to three students get the use of the machine for an entire day (the devices run round the clock). They must connect cables from waveform sources

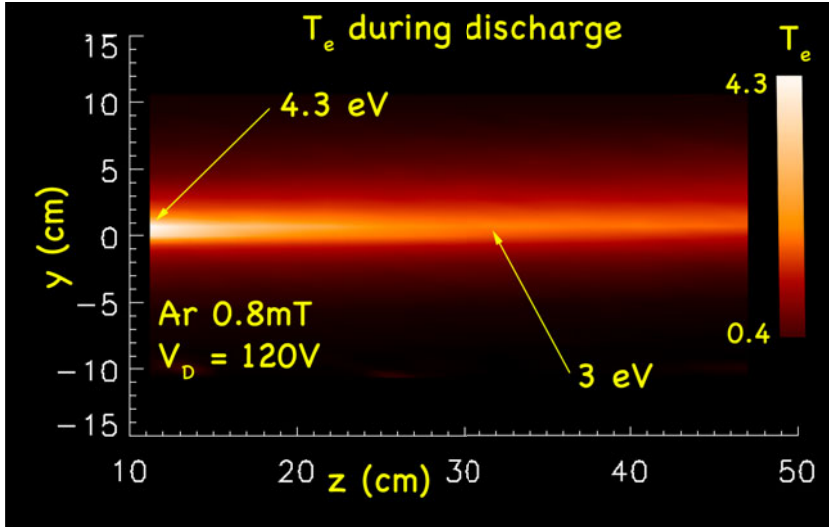


FIGURE 11. Electron temperature measured from  $I$ - $V$  curves during the discharge in the double cathode device. The anode is located at  $z = 0$  and the cathode at  $z = -30$  cm.  $B = 100$  G. The discharge current was 1 Amp.

to antennae, make sure that detectors are working and learn to use the data acquisition system. These are real experiments. Things can go wrong, students can measure the wrong quantity by accident, and probes can break. There is a steep learning curve and the course is time consuming. However, in spite of this, many have commented that it was one of the best courses they took as an undergraduate.

The course has offered a variety of experiments; many more are possible. The device they were done on (ICP or TC-twin cathode device) is called out. This is a list of what has been taught so far:

- (i) Langmuir probe measurements (two-dimensional (2-D) density, temperature and potential) (ICP, TC).
- (ii) Emissive probe determination of 2-D plasma potential (ICP, TC).
- (iii) Electric field measurements of resonance cones. Comparison with theory (ICP).
- (iv) Magnetic field measurements of whistler wave patterns transverse and along the background field. Validation of the Appleton–Hartree equation (ICP).
- (v) Whistler wave ducting in a density depression (ICP).
- (vi) Drift waves (TC).
- (vii) Chaotic waves and deterministic chaos (TC).
- (viii) Instabilities driven by biasing an internal grid (TC).
- (ix) Counter-streaming plasmas (TC).
- (x) Trivelpiece–Gould modes (TC).
- (xi) Ion Bernstein waves (TC).

The course is organized as follows. Each week a lecture on the experiment for the following week is given. These include relevant theory and derivations (for example the resonance cone pattern). Students collect data on their own and there are typically six experiments executed over the 10-week course. Different student groups

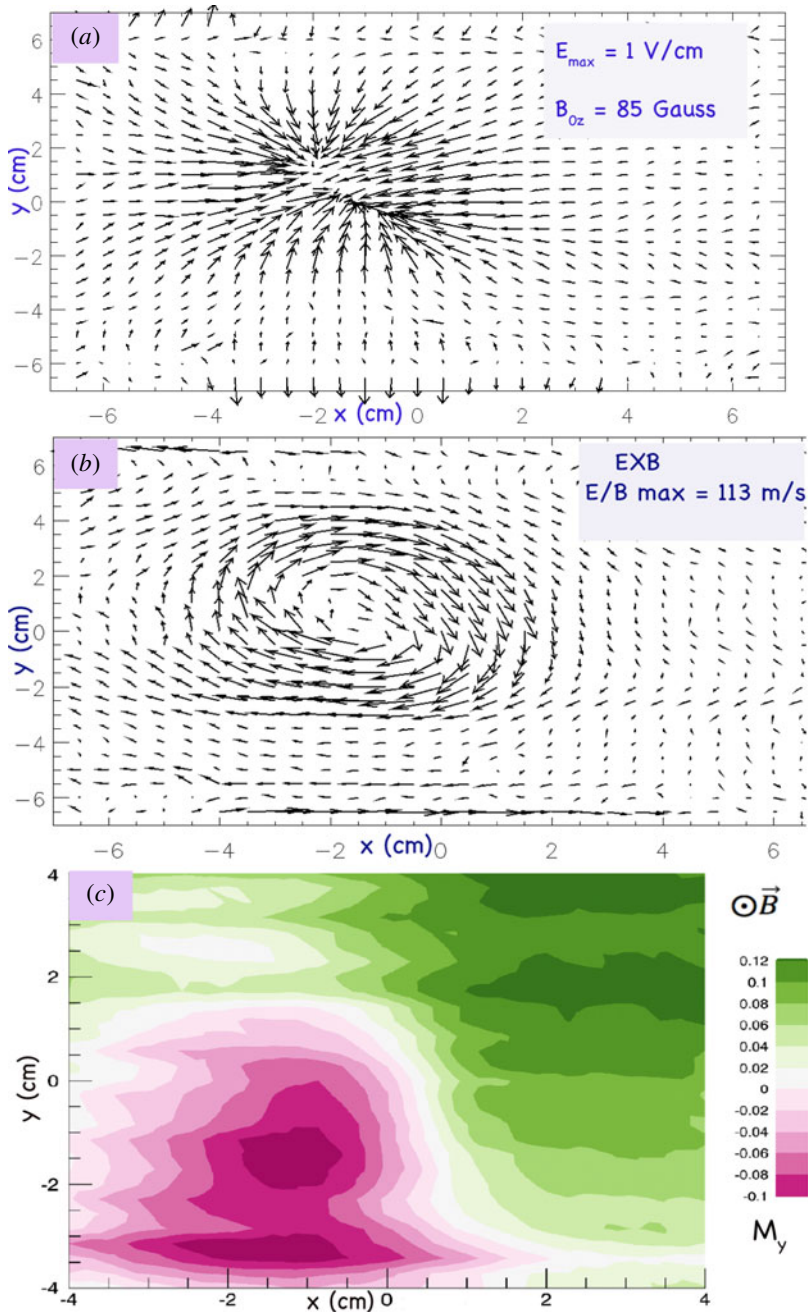


FIGURE 12. (a) Electric field measured from plasma potential acquired from an emissive probe in the afterglow of the dual discharge device ( $T_e = 0.5 \text{ eV}$ ). The magnetic field points into the page. (b) The plasma drift calculated from the electric field. The edge of the plasma rotates which is the case for nearly all plasma columns in a magnetic field. The ion sound speed is  $1.1 \times 10^3 \text{ m s}^{-1}$ . (c) Vertical component of the Mach number on an  $x$ - $y$  plane. The Mach number of 0.1 yields  $v_y = 110 \text{ m s}^{-1}$  in agreement with (b). The Mach probe data were acquired weeks after the emissive probe data with a new  $\text{LaB}_6$  cathode.

are typically assigned different parameters for their experiments and can share huge datasets with each other, allowing mutual collaboration between groups. A laboratory report in the style of a Phys. Rev. Lett. is required for each experiment, co-written by each group. At the end of the quarter, each group gives a 15 min presentation on one of the experiments. The presentations are usually attended by the plasma graduate students in the group as well as the research scientists. Some examples of experimental results are shown below. We highlight two experiments that are performed on the ICP device – whistler waves and resonance cones.

The ICP source operates at 600 kHz and floods the chamber with RF noise. Rather than build frequency compensated probes, experiments in that device are done in the plasma afterglow. When the RF has terminated the electron temperature decays from about 3 eV to below 0.5 eV in approximately 200  $\mu$ s. The density decays slowly, and there is still plasma from the previous pulse when the source is next switched back on 20–90 ms later. The plasma becomes very quiescent in the afterglow with density fluctuations less than one per cent. One can choose the operating density by delaying when the experiment switches on. Different student groups are typically assigned different densities for their experiments. The timing for the whistler wave experiment is shown in figure 13. The timing diagram for the resonance cone experiment is much the same, however, resonance cones are generally launched later in the afterglow than whistlers.

The first experiment studies resonance cones. If an RF signal is applied to a point source in a magnetoplasma the resulting radiation pattern takes the form of double cone (Kuehl 1962; Fisher & Gould 1969). The apex of the cones is at the point source and the central axis is field aligned. The cones occur in two branches the first in which  $\omega < \omega_{pe}$ ,  $\omega_{ce}$  and the second at frequencies  $\omega_{pe}$ ,  $\omega_{ce} < \omega < \sqrt{\omega_{pe}^2 + \omega_{ce}^2}$ . In a cold collisionless plasma, the electric field of the cones is infinite on the surface of the cones, with the cone angle given by

$$\sin^2 \theta = \frac{\omega^2(\omega_{pe}^2 + \omega_{ce}^2 - \omega^2)}{\omega_{pe}^2 \omega_{ce}^2}. \quad (4.1)$$

The experiment was done late in in the afterglow plasma of the ICP device. At this time, the plasma density was low enough ( $n_e \simeq 6 \times 10^8 \text{ cm}^{-3}$ ) to see the cone pattern and prevent the launching of whistler waves. The point source is a 1/8 inch disk attached to the centre conductor of a co-axial cable threaded through a probe shaft into the chamber. The cone pattern was measured using a three axis electric field probe shown in figure 14(a) and the measured transverse electric field of the cone in figure 14(b). The electric field probe consists of six ‘half-dipole’ wires 5 mm in length. The wires are the centre conductors of semi-rigid coaxial cable (e.g. Amawave part no. UT-034-M). The voltages measured by pairs of wires, terminated in 50 Ohms, were subtracted with a low noise, high gain differential amplifier (the circuit diagram is in appendix 3) to give a signal proportional to  $E$ . DC breaks prevent the fine wires from drawing too much current and melting. The total amplifier gain was  $10^4$ . Electric field probes cannot be absolutely calibrated because of the presence of sheaths around the wire tips and in this case the fact that the tips are not accurately measuring fluctuations in the floating potential because of their 50  $\Omega$  impedance. The cones are clearly visible in figure 14(b). Their temporal development is shown in an accompanying movie.

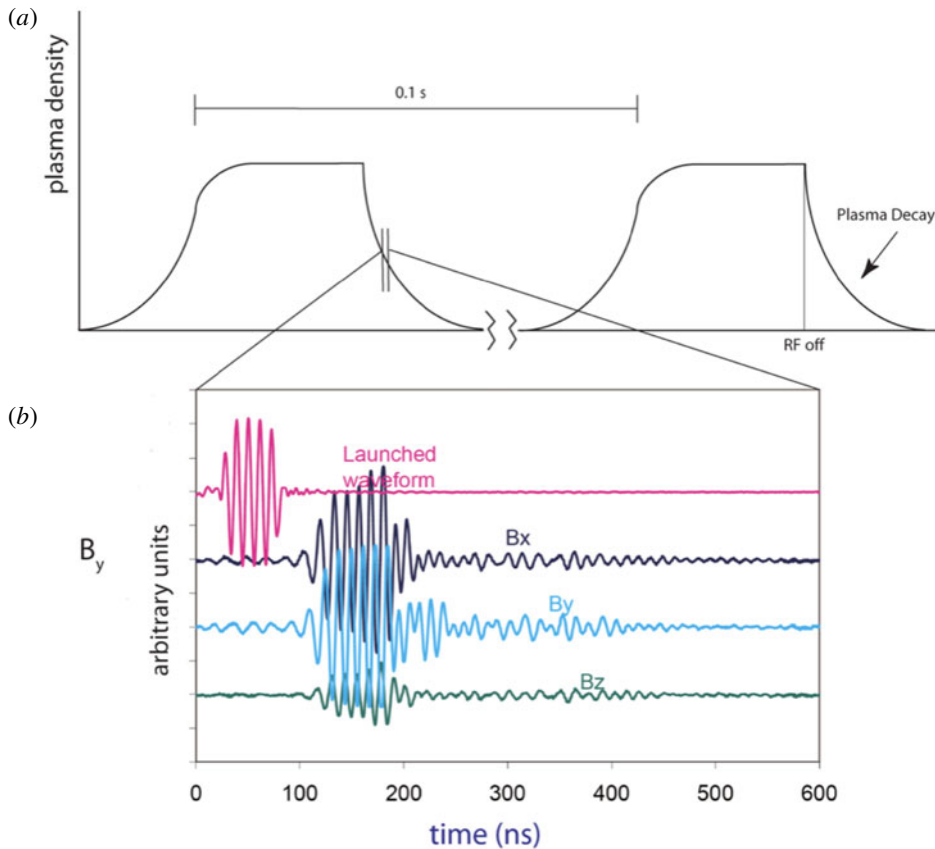


FIGURE 13. (a) Density as a function of time in the pulsed ICP discharge. The experiments can be done during the pulse or in the plasma ‘afterglow’ after the active discharge is switched off. (b) Typical launched and received waveforms of the magnetic field of a whistler wave. The density is essentially constant over the 500 ns time scale of the whistler experiment.

A whistler wave experiment on the ICP device was used to verify the Appleton-Hartree equation (Appleton 1925; Hartree 1931) and measure the whistler wave dispersion relation. Appleton’s equation (4.2) relates the index of refraction  $\eta = kc/\omega$  to the angle of propagation  $\theta$ , the density and magnetic field (in quantities  $\omega_{pe}$ ,  $\omega_{ce}$ ), in a cold plasma where  $\nu$  is the electron neutral collision frequency. A single-turn magnetic loop was used to launch the waves, a schematic of the circuitry for the launcher circuit is shown in figure 15. An arbitrary waveform generator creates a tone burst which is amplified and drives the loop in a push–pull mode. A directional coupler is used to tap off 10% of the signal so it can be recorded by a scope and the data acquisition system. The pulse generator controls the timing: it switches on the RF source and then launches the wave in the plasma afterglow. The magnetic field of the whistler wave is measured using a three axis B-dot probe (Loveberg 1965). Each axis has two oppositely wound half-turns, which are subtracted from one another with a differential amplifier (see appendix II) to remove electrostatic pickup. The signal is then further amplified by a factor of 100 using the same amplifier used

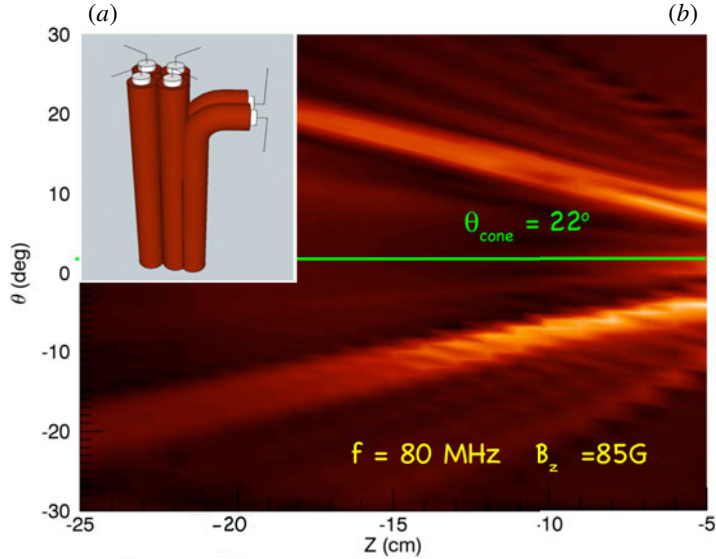


FIGURE 14. (a) Schematic drawing of three-axis high frequency electric dipole probe. Each tip is 5 mm in length. There are six high frequency coaxial cables with SMA connectors on a vacuum feedthrough. (b) Data from the cone angle acquired in the low density afterglow of the ICP plasma. The point source of the cones was a 1/8 inch metal disk at the end of a coaxial feed inside a probe shaft positioned at the origin (i.e.  $x = y = z = 0$ ). The dipole probe cannot be properly calibrated. The brightness of the colour in (b) is proportional to the magnitude of the received signal  $I \propto \sqrt{E_x^2 + E_y^2 + E_z^2}$ .

in the resonance cone experiment.

$$\eta^2 = 1 - \frac{\frac{\omega_{pe}^2}{\omega^2}}{\left(1 + \frac{iv}{\omega}\right) - \frac{\frac{\omega_{ce}^2}{\omega^2} \sin^2 \theta}{2 \left(1 - \frac{\omega_{pe}^2}{\omega^2}\right)} \pm \sqrt{\frac{\left(\frac{\omega_{ce}^2}{\omega^2} \sin^2 \theta\right)^2}{4 \left(1 - \frac{\omega_{pe}^2}{\omega^2}\right)^2} + \frac{\omega_{ce}^2}{\omega^2} \cos^2 \theta}}. \quad (4.2)$$

Whistler wave data from this experiment are shown in figure 16. The waves were launched in the early afterglow (at time  $t = 1$  ms after plasma termination) to ensure the density was high and the parallel wavelengths are short. A movie showing the temporal propagation of the waves is included.

Note that the wave amplitude decreases with distance from the antenna. The observed decay was accurately predicted by (4.2) using the electron neutral collision rate for the damping term  $v$ . The time development of a whistler wave packet at  $f = 100$  MHz and  $B = 80$  G is shown in a supplemental movie.

The whistler experiment was first carried out with a group of high school students in the summer before implementation in the undergraduate laboratory. This resulted in a paper on studying the index of refraction studies in plasmas (Gekelman *et al.* 2011). A second experiment involved the ducting of whistlers into a density minimum.

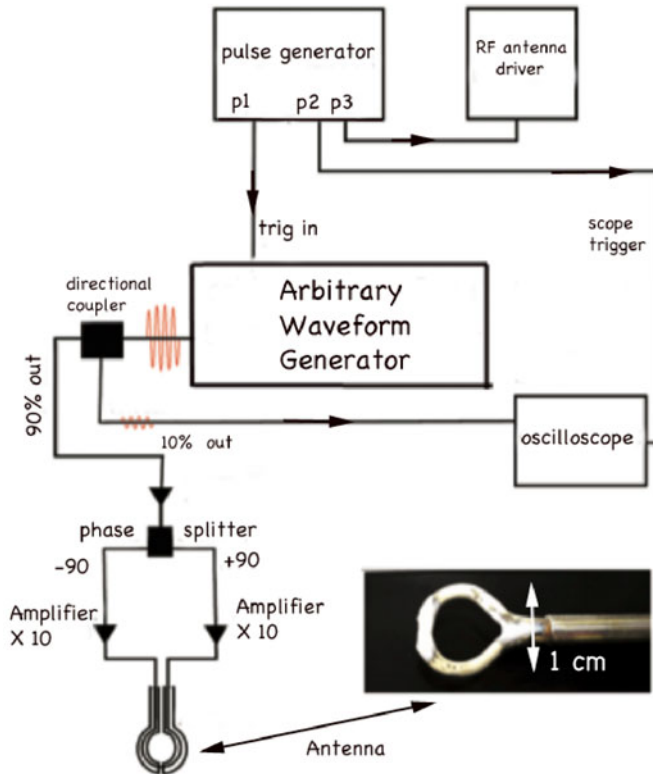


FIGURE 15. The single turn antenna is used in a ‘push–pull’ mode. The tone burst signal is created by the arbitrary waveform generator and then amplified. The signal is then split by a ‘phase splitter’ which generates waveforms that are  $180^\circ$  out of phase. Each output is amplified by a factor of 10. The right arm drives current into the loop and the signal from the left amplifier is negative. Therefore, the loop current is effectively doubled. There is a gap in the outer conductor which allows the signal to escape. The exciter is insulated with epoxy. An advantage of using the anti-symmetric drive scheme is that it imposes a voltage null at the gap in the shield, helping to avoid electrostatic radiated waves (assuming care has been taken to make wire lengths the same on each side).

The density cavity was created by biasing a circular paddle which was placed between the ICP source and the whistler launch. Density striations of 10%–50% could be generated in a helium plasma. The device was used in an experiment that compared a computer simulation to measurements of the ducted wave (Streltsov *et al.* 2012). This illustrates that it is possible to do research in these devices apart from using them as teaching tools.

## 5. Laboratory safety

Laboratory safety is a key issue for any course involving students who may have little or no experience with the type of equipment described here. There are two locations in the 180E lab that can pose an electrical shock hazard. The first is the ICP source which has an RF voltage of hundreds of volts. The RF is on for 5–10 ms at a 10 Hz repetition rate. There is no applied voltage during the off time.

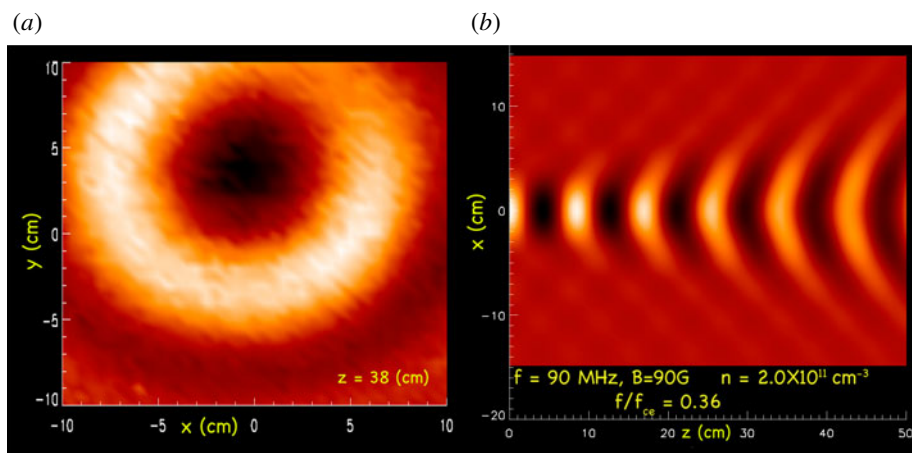


FIGURE 16. Measured whistler wave patterns in a helium plasma. (a) Amplitude of whistler waves in a plane transverse to the background magnetic field at  $z = 38$  cm from the launch point. (b) Whistler wave component  $B_y$  as a function of distance from the antenna (located at  $z = 0$ ). The bright areas are wave maxima and the dark minima. Note that the transverse probe was misaligned and the antenna is located at  $y = 4$  cm in (a). The parallel wavelength from (b) is 10 cm.

However, touching one of the electrodes may lead to a shock and possibly an RF burn. To protect the students, the entire ICP source is enclosed in a plexiglass box with ‘Danger High Voltage’ signs on all sides (see figure 2). The second shock hazard is the twin cathode device in which the voltage between the cathodes and anodes can go up to 120 Volts. These are pulsed on for 5–10 ms and the anodes of both sources are grounded. The connection to both cathodes, which are pulsed negatively with respect to the anodes, are insulated as are the wires that go from the transistor switches and their associated capacitor banks. The capacitors and transistors are in an enclosed box housed underneath the machine. One would have to work very hard to get to them. The rest of the equipment utilized in the laboratory contain low voltages and is harmless. The cathodes run at elevated temperatures but they are in the machine and cannot be touched. Since they are relatively small, the walls of the device do not heat up and there is not a burn hazard. There is a laboratory orientation on the first day of class where the students are shown all the machine components and given a safety lecture. The current 180E lab course has been offered twice a year for the past six years. Previous versions of the laboratory have run for at least three decades. There has never been a serious accident.

## 6. Summary and conclusions

This paper is a step by step guide to building an undergraduate (or graduate) plasma physics instructional laboratory. The cost of the RF powered device (one of the two described) is of the order of \$40 000 (USD). This does not include a digital oscilloscope for viewing and acquiring data and a computer for storing the data acquisition software and experimental data reside. Additional computers to analyse data are useful, but also not included. The cost of these with additional measurement equipment would increase the price. Additional equipment for the laboratory is acquired over the years from awards, in this case the UCLA Office of

Instructional Development was a great help. The twin cathode DC discharge machine is comparable in cost. One must also factor in the upkeep and repair costs which can amount to \$10 000/year. This is a substantial investment but it is on par with the cost of other labs such as those geared to study quantum entanglement or low temperature physics. The UCLA physics department has hosted a plasma laboratory course for decades. The current version described in this manuscript has been running smoothly for the past six years and is currently taught twice a year. We have not tracked all the students but several have gone on to get a doctorate in Physics or Engineering at UCLA and at other institutions (e.g. Princeton, MIT, USC, CalTech). The students evaluate the course at the end of the quarter. In general, the evaluations state that the course is difficult and time consuming, but it is arguably one of the best courses they had as an undergraduate at UCLA. There are several cases of students deciding to go into plasma physics after having taken Physics 180E. Plasma physics addresses a large variety of fundamental topics such as nonlinear phenomena, turbulence and a host of waves which interact with one another. It also has a host of important real world applications such as thermonuclear fusion, space weather, plasma processing and plasma medicine to name a few. Laboratories such as this are important for the training of the next generation of plasma scientists.

#### **Data Availability Statement**

The data that support the findings of this study are available within the article and its supplementary material.

#### **Acknowledgements**

The authors would like to thank the UCLA Physics Department for its continuing monetary support of the 180E Plasma Lab. Funds for the oscilloscopes and several power supplies were generously provided by the UCLA Office of Instructional Development as mini grants for education. We especially thank the Ahmanson Foundation and board member Mr J. Wagner for donating funds to fabricate the ICP device. We also appreciate the expert help of T. Ly and M. Drandell for their expert technical assistance. The development of this lab owes a great deal to the environment provided by the Basic Plasma Science Facility, which is jointly funded by the Department of Energy (DOE) Office of Fusion Energy Science and the Physics division of the National Science Foundation (NSF). We finally thank all the 180E students whose hard work and enthusiasm made the course rewarding to teach.

*Editor Harmut Zohm thanks the referees for their advice in evaluating this article.*

#### **Supplementary movies**

Supplementary movies are available at <https://doi.org/10.1017/S002237782000063X>.

#### REFERENCES

- ALEXEFF, I., PYTLINSKI, J. T. & OLESON, N. L. 1977 New elementary experiments in plasma physics. *Am. J. Phys.* **45** (9), 860–866.
- APPLETON, E. V. 1925 Geophysical influences on the transmission of wireless waves. *Proc. Phys. Soc.* **37**, 16D.

- CHEN, F. F., ETIEVANT, C. & MOSHER, D. 1968 Measurement of low plasma densities in a magnetic field. *Phys. Fluids* **11**, 811.
- CRAWFORD, F. W. & ILIC, D. B. 1976 Laboratory course in plasma physics. *Am. J. Phys.* **44** (4), 319–326.
- FISHER, R. K. & GOULD, R. W. 1969 Resonance cones in the field pattern of a short antenna in an anisotropic plasma. *Phys. Rev. Lett.* **22**, 1093.
- FLEDDERMANN, C. B. 1997 Plasma etching and plasma physics experiments for the undergraduate microelectronics course. *IEEE Trans. Educ.* **40**, 207–212.
- GEKELMAN, W., PRIBYL, P., WISE, J., LEE, A., HWANG, R., EGHTEBAS, C., SHIN, J. & BAKER, B. 2011 Using plasma experiments to illustrate a complex index of refraction. *Am. J. Phys.* **79** (9), 894.
- GILMORE, M., GEKELMAN, W., REILING, K. & PEEBLES, W. A. A reliable millimeter-wave quadrature interferometer. [arXiv:2002.11190](https://arxiv.org/abs/2002.11190). On archive only, unpublished in a peer reviewed journal.
- HARTREE, D. R. 1931 The propagation of electromagnetic waves in a refracting medium in a magnetic field. *Proc. Camb. Phil. Soc.* **27**, 143.
- HERSHKOWITZ, N. 1989 How Langmuir probes work. In *Plasma Diagnostics: Discharge Parameters and Chemistry* (ed. O. Auciello & D. L. Flamm), p. 113. Academic Press.
- HUTCHINSON, I. 2002 Plasma mach probes with unmagnetized ions. In *29th EPS Conference on Plasma Physics and Contr. Fusion, Montreux, ECA*, vol. 26B, 1.004. Plasma Phys. and Control. Fusion.
- KABOT, L. R., WORDEN, T. M., MATSUSHITA, A. K., HERNANDEZ, R. X. & ABRAMZON, N. 2016 Inquiry base experiment: the effect of plasma on glass surface properties. *Intl J. Eng. Pedagogy* **6**, 65–67.
- KUEHL, H. H. 1962 Electromagnetic radiation from an electric dipole in a cold anisotropic plasma. *Phys. Fluids* **5**, 1095.
- LENEMAN, D. & GEKELMAN, W. 2001 A novel angular motion feedthrough. *Rev. Sci. Instrum.* **72**, 3473–3474.
- LOVEBERG, R. H. 1965 Magnetic probes. In *Plasma Diagnostic Techniques* (ed. R. Huddleston & S. Leonard), p. 69. Academic Press.
- MACLATCHY, C. S. 1977 A low-cost experiment in plasma physics for the advanced undergraduate lab. *Am. J. Phys.* **45** (10), 910–913.
- MOTT SMITH, H. & LANGMUIR, I. 1926 The theory of collectors in gaseous discharges. *Phys. Rev. B* **28**, 727.
- SHEEHAN, J. P., RAITSES, Y., HERSHKOWITZ, N., KRAGANOVICH, I. & FISCH, N. J. 2011 A comparison of emissive probe techniques for electric potential measurements in a complex plasma. *Phys. Plasmas* **18**, 073501.
- STRELTSOV, A., WOODROFFE, J., GEKELMAN, W. & PRIBYL, P. 2012 Modeling the propagation of whistler-mode waves in the presence of field-aligned density striations. *Phys. Plasmas* **19**, 102104.
- WISSEL, S. A., ZWICKER, A., ROSS, J. & GERSHMAN, S. 2013 The use of dc glow discharges as undergraduate education tools. *Am. J. Phys.* **81** (9), 663–669.